

Special issue “The advance of solid tumor research in China”: 68Ga-PSMA-11 PET/CT for evaluating primary and metastatic lesions in different histological subtypes of renal cell carcinoma

Yilin Li¹ | Rongliang Zheng² | Yijun Zhang³ | Chaoyun Huang³ | Li Tian⁴ |
 Ruiqi Liu¹  | Yang Liu¹ | Zhiling Zhang⁵ | Hui Han⁵ | Fangjian Zhou⁵ |
 Liru He¹  | Pei Dong⁵ 

¹Department of Radiation Oncology, Sun Yat-sen University Cancer Center, State Key Laboratory of Oncology in South China, Collaborative Innovation Center for Cancer Medicine, Guangzhou, People's Republic of China

²Department of Nuclear Medicine, Sun Yat-sen University Cancer Center, State Key Laboratory of Oncology in South China, Collaborative Innovation Center for Cancer Medicine, Guangzhou, People's Republic of China

³Department of Pathology, Sun Yat-sen University Cancer Center, State Key Laboratory of Oncology in South China, Collaborative Innovation Center for Cancer Medicine, Guangzhou, People's Republic of China

⁴Department of Radiology, Sun Yat-sen University Cancer Center, State Key Laboratory of Oncology in South China, Collaborative Innovation Center for Cancer Medicine, Guangzhou, People's Republic of China

⁵Department of Urology, Sun Yat-sen University Cancer Center, State Key Laboratory of Oncology in South China, Collaborative Innovation Center for Cancer Medicine, Guangzhou, People's Republic of China

Correspondence

Liru He, Department of Radiation Oncology
 Sun Yat-sen University Cancer Center, State
 Key Laboratory of Oncology in South China,
 Collaborative Innovation Center for
 Cancer Medicine 651 Dongfeng Road East,
 Guangzhou 510060, People's Republic
 of China.

Email: helir@sysucc.org.cn

Pei Dong, Department of Urology, Sun Yat-sen
 University Cancer Center, State Key
 Laboratory of Oncology in South China,
 Collaborative Innovation Center for Cancer
 Medicine, 651 Dongfeng Road East,
 Guangzhou 510060, People's Republic of
 China.

Email: dongpei@sysucc.org.cn

Funding information

National Natural Science Foundation of China,
 Grant/Award Number: 81772483

Abstract

Conventional imaging examinations are not sensitive enough for the early detection of recurrent or metastatic lesions in renal cell carcinoma (RCC) patients. We aimed to explore the role of ⁶⁸Ga-prostate specific membrane antigen (PSMA)-11 positron emission tomography (PET)/computed tomography (CT) in the detection of primary and metastatic lesions in such patients. We retrospectively analyzed 50 RCC patients who underwent ⁶⁸Ga-PSMA-11 PET/CT from November 2017 to December 2020. We observed a higher median accuracy and tumor-to-background maximum standard uptake value (SUV_{max}) ratio (TBR) of ⁶⁸Ga-PSMA-11 PET/CT in clear cell RCC (ccRCC; 96.57% and 6.00, respectively) than in non-clear cell RCC (ncRCC; 82.05% and 2.99, respectively). The accuracies in detecting lesions in the renal region, bone, lymph nodes and lungs in ccRCC were 100.00%, 95.00%, 98.08% and 75.00%, respectively, and those in the renal region, bone and lymph nodes in ncRCC were 100.00%, 86.67% and 36.36%, respectively. The median TBRs of the lesions from the

Abbreviations: ⁶⁸Ga, Gallium-68; BS, bone scan; ccRCC, clear cell renal cell carcinoma; CT, computed tomography; HE, hematoxylin and eosin; IHC, immunohistochemistry; MRI, magnetic resonance imaging; ncRCC, non-clear cell renal cell carcinoma; PET, positron emission tomography; PSMA, prostate-specific membrane antigen; RCC, renal cell carcinoma; SUV, standard uptake value; SUV_{max}, maximum standard uptake value; T1-w, T1-weighted; T2-w, T2-weighted; TBR, tumor-to-background maximum standard uptake value ratio; US, ultrasound; WHO, World Health Organization.

Yilin Li, Rongliang Zheng and Yijun Zhang have contributed equally to this study.

This is an open access article under the terms of the [Creative Commons Attribution-NonCommercial-NoDerivs](https://creativecommons.org/licenses/by-nc-nd/4.0/) License, which permits use and distribution in any medium, provided the original work is properly cited, the use is non-commercial and no modifications or adaptations are made.

© 2022 The Authors. *International Journal of Cancer* published by John Wiley & Sons Ltd on behalf of UICC.

above locations were 0.38, 10.96, 6.69 and 13.71, respectively, in ccRCC and 0.13, 4.02 and 0.73, respectively, in ncRCC. The PSMA score evaluated with immunohistochemistry was correlated with the SUV_{max} ($P = .046$) in RCC. Higher PSMA scores were observed in ccRCC than in ncRCC ($P = .031$). ^{68}Ga -PSMA-11 PET/CT resulted in changes in clinical management in 12.9% (4/31) of cases because of the discovery of new metastases not detected with conventional imaging. These results indicate that ^{68}Ga -PSMA-11 PET/CT is a promising method for the detection of metastatic lesions in ccRCC, especially for those in the bone and lymph nodes.

KEYWORDS

^{68}Ga -PSMA-11 PET/CT, accuracy, cancer staging, renal cell carcinoma, tumor-to-background SUV_{max} ratio

What's new?

Accurate staging and assessment of metastases are important in guiding clinical treatment of patients with renal cell carcinoma (RCC). Early detection of metastatic lesions in RCC, however, presents unique challenges, owing to small lesion size, which escapes conventional imaging. Here, the authors investigated ^{68}Ga -PSMA-11, a positron emission tomography (PET) ligand targeted toward prostate-specific membrane antigen (PSMA) in the tumor neovasculature, for the detection of RCC lesions. Compared with conventional imaging, ^{68}Ga -PSMA-11 PET/CT exhibited superior sensitivity and accuracy in metastatic lesion detection in clear cell RCC. Accuracy in the detection of lesions in the lymph nodes and bone was notably high.

1 | INTRODUCTION

In 2020, renal cell carcinoma (RCC) was the ninth most frequently diagnosed cancer in men and the 14th most frequently diagnosed cancer in women worldwide.¹ Accurate staging and assessment of metastases are important for the guidance of clinical treatment. Traditionally, ultrasound (US), computed tomography (CT), magnetic resonance imaging (MRI) and bone scanning (BS) have been used to detect and characterize renal masses and metastases.²⁻⁵ However, in the early phases of metastatic disease, none of these are sensitive enough for the comprehensive detection of small metastatic lesions.⁶ There is, therefore, an urgent need for more sensitive and specific imaging technologies for the early detection of metastases for accurate staging and timely treatment of RCC.

Prostate-specific membrane antigen (PSMA) is a type II integral membrane glycoprotein of approximately 100 kDa that was originally considered prostate-specific, but was subsequently shown to be present on many other normal and pathological tissues, such as the neovasculature of many tumor types, including RCC.⁷⁻⁹ Thus, the different endothelial expression of PSMA by tumor neovasculature is a potential target in RCC. Positron emission tomography (PET) with ligands of PSMA (eg, ^{68}Ga -PSMA-11) is a relatively new nuclear imaging modality with great potential, and has been applied in prostate cancer management.¹⁰⁻¹³ More recently, the clinical use of ^{68}Ga -PSMA-11 PET/CT for the improved detection of RCC lesions has gained interest, as is clear from the publication of several case reports and retrospective studies with small samples.¹⁴⁻²¹

However, the difference in detection rates of primary and metastatic lesions by ^{68}Ga -PSMA-11 PET/CT in RCC remains unclear, and its clinical indications for RCC are yet to be identified. Thus, we aimed to explore the role of ^{68}Ga -PSMA-11 PET/CT in the detection of primary and metastatic lesions in different histological subtypes of RCC.

2 | MATERIALS AND METHODS

2.1 | Patients

This was a retrospective case series at a single tertiary institution between November 2017 and December 2020. The inclusion criteria were as follows: (1) pathological diagnosis of RCC, (2) at least one ^{68}Ga -PSMA-11 PET/CT scan and (3) at least three radiographical follow-ups every 3 months after ^{68}Ga -PSMA-11 PET/CT. Considering that increasing attention has been paid in recent years to the local treatment of patients with 5 to 10 metastases,^{22,23} we selected patients with ≤ 10 lesions for statistical analysis by lesions. The exclusion criteria were as follows: (1) previous or sequential second primary cancers, (2) incomplete medical records, including follow-up, or (3) with more than 10 lesions, without contemporaneous CT or MRI (within 1 month), and without tissue samples sufficient by surgery or biopsy (within 1 month). All reported investigations were conducted in accordance with the Declaration of Helsinki and national regulations.

2.2 | ⁶⁸Ga-PSMA-11 PET/CT examination

Whole-body scans were performed by using a combined PET/CT system (Siemens Biograph mCT.X, Siemens AG, Munich, Germany). Patients did not need to fast before the examination but had to drink 500 ml of water within 2 h to ensure sufficient hydration. To reduce urinary radioactivity, the bladder was emptied before imaging. Whole-body images were collected 60 to 90 min after injection of 0.05 mCi/kg ⁶⁸Ga-PSMA-11. The scanning range was from the base of the skull to the middle of the femur, and local collection was performed if necessary. Low-dose CT-scanning was mainly used for attenuation correction and lesion localization in PET images. Automatic milliampere-control technology was used for diagnostic CT scanning. PET was conducted in 3D mode for 3 min per bed position. If the lesion was not clear in the initial images, delayed imaging was performed 3 to 4 h later. A syngo TrueD (Siemens AG) workstation was used for the registration and fusion of the acquired images from the PET and CT scans. Corrections were applied for random effects, geometry, attenuation and scatter.

2.3 | Conventional imaging examination

CT: All patients received enhanced chest, abdomen and pelvis CT. Patients received were administered a peripheral intravenous injection of nonionic iodinated contrast material (300 mg/ml) via a high-pressure injector at a flow rate of 2.5 to 3.0 ml/s and a total dose of 80 to 100 ml (1.0 ml/kg) after non-enhanced CT. The corticomedullary, nephrographic and excretory phases were started 30, 60 and 180 s, respectively, after intravenous injection of the contrast agent.

MRI: MRI was performed for lesions requiring additional attention, such as bone metastases and brain metastases. The MRI protocol comprised coronal turbo inversion recovery, axial T1-weighted (T1-w), axial T2-w and diffusion-weighted sequences, with *b*-values of 0 and 800 s/mm² in the axial plane. After gadolinium injection, T1-w fat-saturated sequences were obtained in the axial and coronal planes.

2.4 | Imaging analysis

The original images obtained via PET/CT, CT and MRI were individually analyzed by two nuclear medicine physicians (Rongliang Zheng and Wen Long) and two radiologists (Li Tian and Huali Ma) who were blinded to the clinical history of the patients. Any images resulting in different opinions were reevaluated by all four experts until a consensus was reached. Oligometastasis was defined as no more than five metastatic lesions. The intensity of ⁶⁸Ga-PSMA uptake was assessed based on the standard uptake value (SUV). The maximum SUV (SUV_{max}) was recorded as a statistical criterion to minimize partial volume effects and improve reproducibility of the measurements. A positive PET/CT scan was defined as containing a moderate or intense PSMA-avid lesion with an SUV_{max} ≥ 2 as reported.¹⁹ The lesion was considered true positive if histopathology showed RCC or at least two

of the following criteria were met: (1) the lesion showed typical appearance on two or more imaging examinations; (2) the lesion increased in size from one imaging exam to the next; (3) the lesion decreased in size from one imaging exam to the next, following appropriate treatment and (4) the lesion was associated with clinical symptoms suggesting malignancy.²⁴ The lesion was considered true negative if it was pathologically confirmed or had no significant changes after at least 6 months of follow-up. The lesion was considered true negative if it was pathologically confirmed, or it did not have typical appearance by imaging examinations and significant changes after at least 9 months of follow-up.^{25,26} Tumor-to-background ratios (TBRs), calculated by dividing the SUV_{max} of the tumor by the SUV_{max} of the background tissue, were determined to quantify the image contrast. TBRs were calculated for the primary tumor (relative to morphologically unaltered renal parenchyma) and metastases in the lymph nodes (relative to soft tissue), bone (relative to bone spongiosa), the lungs (relative to lung parenchyma), the liver (relative to liver parenchyma) and soft-tissue nodules (relative to nearby soft tissue).^{17,27}

2.5 | Histopathological analysis

Renal tumor specimens were sectioned, fixed and subjected to paraffin embedding and hematoxylin and eosin (HE) staining. All sections were reviewed, and consensus was obtained by two urological pathologists according to the 2016 World Health Organization (WHO) classification of tumors of the urinary system and male genital organs.²⁸ HE staining was used to determine the pathological PSMA expression. Briefly, 5 μm tissue sections were deparaffinized in xylene, rehydrated through a graded alcohol series, immersed in 3% hydrogen peroxide for 10 min to block endogenous peroxidase activity, and subjected to antigen retrieval by pressure cooking for 3 min in citrate buffer (pH 6.0). The slides were subsequently incubated with 10% normal goat serum at room temperature for 30 min to reduce nonspecific reactivity. Thereafter, they were incubated sequentially with primary anti-PSMA antibody (#12815; Cell Signaling Technology, Danvers, MA; 1:100 dilution) overnight at 4°C, incubated with a secondary antibody (Envision; Dako, Glostrup, Denmark) for 1 h at room temperature, washed twice with phosphate buffered saline for 5 min, and developed by using 3,3'-diaminobenzidine. Finally, the sections were counterstained with Mayer's hematoxylin, dehydrated and mounted. Negative controls were prepared by replacing the primary antibody with normal murine immunoglobulin G.

PSMA is mainly expressed in the endothelial cells of tumor-associated neovasculature in RCC.²⁹ The average density (number of PSMA-positive neovasculatures/high-power field) was quantitatively scored by two pathologists (Yijun Zhang and Ping Yang). Five fields of view (magnification ×400) were randomly selected in tumor-tissue areas, the absolute number of PSMA-positive neovasculatures was counted in each, and the average was calculated. The immunohistochemistry (IHC) score was obtained by multiplying the score for the average density of positively stained neovasculatures ("1" < median number of positive neovasculatures and "2" ≥ median number of positive neovasculatures) according to the staining-intensity score

(“0” negative staining, “1” [weak staining], “2” moderate staining and “3” strong staining) to obtain the final score for each section.³⁰

2.6 | Analysis

IBM SPSS Statistics for Windows version 22.0 (IBM Corp., Armonk, NY) was used for the statistical analysis. The sensitivity, specificity, accuracy and TBR of ⁶⁸Ga-PSMA-11 PET/CT in detecting different RCC lesions were also calculated. Accuracy = (true negatives + true positives)/total number. Values of radiological parameters were compared within different subgroups using Student's *t* test. Statistical significance was set at *P* < .05.

3 | RESULTS

3.1 | Patient characteristics

There were 36 patients whose ⁶⁸Ga-PSMA-11 PET/CT scan showed no more than 10 lesions. We retrospectively collected these ⁶⁸Ga-PSMA-11 PET/CT scans to analyze the accuracy of different pathological types and sites. We also retrospectively collected 31 ⁶⁸Ga-PSMA-11 PET/CT scans from 31 patients who underwent contemporaneous CT or MRI (within 1 month of ⁶⁸Ga-PSMA-11 PET/CT scan) to analyze the changes in management due to ⁶⁸Ga-PSMA-11 PET/CT. A total of 50 RCC patients were included in the analysis, since there were 17 patients with no more than 10 lesions and contemporaneous images. Of these 50 patients, only nine patients were able to obtain sufficient contemporaneous surgery or biopsy pathological samples for IHC (within 1 month of ⁶⁸Ga-PSMA-11 PET/CT scan). We retrospectively collected these nine ⁶⁸Ga-PSMA-11 PET/CT scans and unstained pathological sections to analyze the relationship between PSMA score and SUV_{max}.

The median age of these 50 patients was 55 years. Forty (80%) cases were diagnosed as clear cell RCC (ccRCC), three papillary renal cell carcinoma, two MIT family translocation RCC, one chromophobe RCC, one mucinous tubular and spindle cell carcinoma, one poorly differentiated RCC, and two others. Forty-one cases were metastatic RCC, 20 of which were oligometastatic. The other nine patients underwent ⁶⁸Ga-PSMA-11 PET/CT scans after nephrectomy, of which six were negative and three exhibited recurrences. Lesions were detected in the following locations: the renal region (*n* = 16), lymph nodes (*n* = 17), bone (*n* = 25), lungs (*n* = 13) and other (*n* = 17) (Table 1).

3.2 | Imaging characteristics for patients with no more than 10 lesions

Thirty-six of the 50 patients had no more than 10 lesions, and the total number of lesions was 94. Among them, 60 lesions were diagnosed as ccRCC (Table 2).

The median SUV_{max} and TBR were higher for lesions in ccRCC (9.0 and 6.00, respectively) than in nonclear cell RCC (ncRCC) (3.7 and 2.99, respectively). The accuracy, sensitivity and specificity were

TABLE 1 Baseline characteristics for the whole cohort

	Patients (<i>n</i> = 50)	Patients with no more than 10 lesions (<i>n</i> = 36)	Patients with contemporaneous CT/MRI scans (<i>n</i> = 31)
Sex			
Male	39	27	24
Female	11	9	7
Age			
Median (IQR)	55 (47-64)	58 (48-65)	54 (47-64)
Negative			
	6	6	2
Positive			
Local	3	3	2
Oligometastases	20	20	10
Multiple metastases	21	7	17
Location			
Renal region	16	8	13
Lymph node	17	9	12
Bone	25	13	18
Lungs	13	8	8
Other ^a	17	10	12
Pathological type			
Clear cell	40	29	23
Nonclear cell	10	7	8

Abbreviations: CT, computed tomography; IQR, interquartile range; MRI, magnetic resonance imaging.

^aEight patients with soft-tissue nodules in the abdominal cavity, five with adrenal metastases, three with soft-tissue nodules in the pelvic cavity, three with liver metastases, one with a soft-tissue nodule in the thoracic cavity and one with brain metastasis.

higher in ccRCC (96.57%, 93.65% and 97.87%, respectively) than in ncRCC (82.05%, 70.59% and 90.91%, respectively).

The median SUV_{max} was higher in primary tumors (16.8) than in metastatic lesions (3.7-9.6), while the median TBRs were higher in metastatic lesions (2.13-13.71) than in primary tumors (0.33). The accuracies, sensitivities and specificities of ⁶⁸Ga-PSMA-11 PET/CT in detecting different metastatic lesions were 75.00%-93.48%, 61.90%-94.59% and 87.50%-100.00%, respectively.

3.3 | Imaging characteristics for different pathological types

We explored the differences in the detection of lesions in ccRCC and ncRCC with ⁶⁸Ga-PSMA-11 PET/CT by analyzing SUV_{max} and TBR values (Table 3). In each location, both the median SUV_{max} and TBR were higher in ccRCC than those in ncRCC. The median TBRs were higher in metastatic lesions than in primary tumors in both ccRCC (6.03-13.71 vs 0.38) and ncRCC (0.73-4.02 vs 0.13).

TABLE 2 Diagnostic values of ^{68}Ga -PSMA-11 PET/CT

	Lesions n = 94	D_{max} median (IQR) (cm)	SUV_{max} median	TBR median	Accuracy (%)	Sensitivity (%)	Specificity (%)
Pathological type							
Clear cell	60	2.1 (1.3-3.0)	9.0	6.00	96.57	93.65%	97.87%
Nonclear cell	34	1.8 (1.1-2.5)	3.7	2.99	82.05	70.59	90.91
Location							
Renal region	10	3.9 (3.0-9.6)	16.8	0.33	100.00	100.00	100.00
Lymph node	21	1.8 (1.5-2.1)	3.7	2.13	92.17	61.90	98.94
Bone	37	2.0 (0.9-2.5)	5.4	4.81	90.59	94.59	87.50
Lungs	7	1.6 (1.3-2.0)	9.6	13.71	75.00	71.43	100.00
Other ^a	19	1.9 (0.9-2.8)	6.8	6.00	93.48	85.00	100.00

Abbreviations: CT, computed tomography; D_{max} , maximum diameter; ^{68}Ga , gallium-68; PET, positron emission tomography; PSMA, prostate-specific membrane antigen; SUV_{max} , maximum standard uptake value; TBR, tumor-to-background maximum standard uptake value ratio.

^aSeven adrenal metastases, seven soft-tissue nodules in the abdominal cavity, two soft-tissue nodules in the pelvic cavity, two brain metastases and one liver metastasis.

TABLE 3 Diagnostic values of ^{68}Ga -PSMA-11 PET/CT in different pathological types

	Lesions	D_{max} median (IQR) (cm)	SUV_{max} median	TBR median	Accuracy (%)	Sensitivity (%)	Specificity (%)
Clear cell							
Renal region	9	3.9 (2.7-7.9)	18.0	0.38	100.00	100.00	100.00
Lymph node	14	1.9 (1.5-2.2)	9.6	6.69	98.08	92.86	98.89
Bone	19	1.9 (0.8-2.2)	7.5	10.96	95.00	100.00	90.48
Lungs	7	1.6 (1.3-2.0)	9.6	13.71	75.00	71.43	100.00
Other ^a	11	2.4 (1.3-2.8)	7.4	6.03	93.33	83.33	100.00
Nonclear cell							
Renal region	1	10.2 (10.2-10.2)	4.9	0.13	100.00	100.00	100.00
Lymph node	7	1.8 (1.5-1.9)	0.7	0.73	36.36	0.00	100.00
Bone	18	2.4 (1.5-2.5)	4.2	4.02	86.67	88.89	85.19
Other ^b	8	1.2 (0.8-2.2)	4.9	3.92	93.75	87.50	100.00

Abbreviations: CT, computed tomography; D_{max} , maximum diameter; ^{68}Ga , gallium-68; PET, positron emission tomography; PSMA, prostate-specific membrane; SUV_{max} , maximum standard uptake value; TBR, tumor-to-background maximum standard uptake value ratio.

^aSix adrenal metastases, three soft-tissue nodules in the abdominal cavity and two brain metastases.

^bFour soft-tissue nodules in the abdominal cavity, two soft-tissue nodules in the pelvic cavity, one adrenal metastasis and one liver metastasis.

In ccRCC, the accuracies of ^{68}Ga -PSMA-11 PET/CT in detecting lesions in different locations were above 90%, except for in the lungs (75.00%). Their sensitivities were above 80%, except for detecting lesions in the lungs (71.43%), while all the specificities were all above 90%. In ncRCC, the accuracies of ^{68}Ga -PSMA-11 PET/CT in detecting lesions in lymph nodes and bone were 36.36% and 86.67%, respectively. The sensitivities in detecting metastatic lesions were all below 90%.

3.4 | Association of imaging characteristics and pathological characteristics

Hematoxylin and eosin (HE) staining and IHC were implemented in the nine patients who underwent surgery or biopsy at the same time that they underwent ^{68}Ga -PSMA-11 PET/CT (Table S1). PSMA expression was observed in tumor-associated neovasculature, and eight of the nine cases

exhibited different PSMA-expression intensity and different density in neovasculature. Only one sample exhibited negative PSMA staining.

In the nine samples, seven were pathologically diagnosed as ccRCC, while five were from metastatic lesions. The SUV_{max} values are related to the pathologic types and PSMA scores (Figure 1). The mean PSMA score and mean SUV_{max} were 3.9 ± 1.9 and 12.5 ± 10.0 , respectively, in ccRCC, while those in ncRCC were 1.5 ± 0.5 and 3.6 ± 2.5 , respectively. Student's t-test revealed that the PSMA score of ccRCC was significantly higher than that of ncRCC ($P = .008$), and the PSMA score was significantly correlated with SUV_{max} in RCC samples ($P = .035$).

3.5 | Heterogeneity in different imaging examinations

Overall, 31 of the 50 patients underwent contemporaneous CT/MRI within 1 month before or after ^{68}Ga -PSMA-11 PET/CT. Among them,

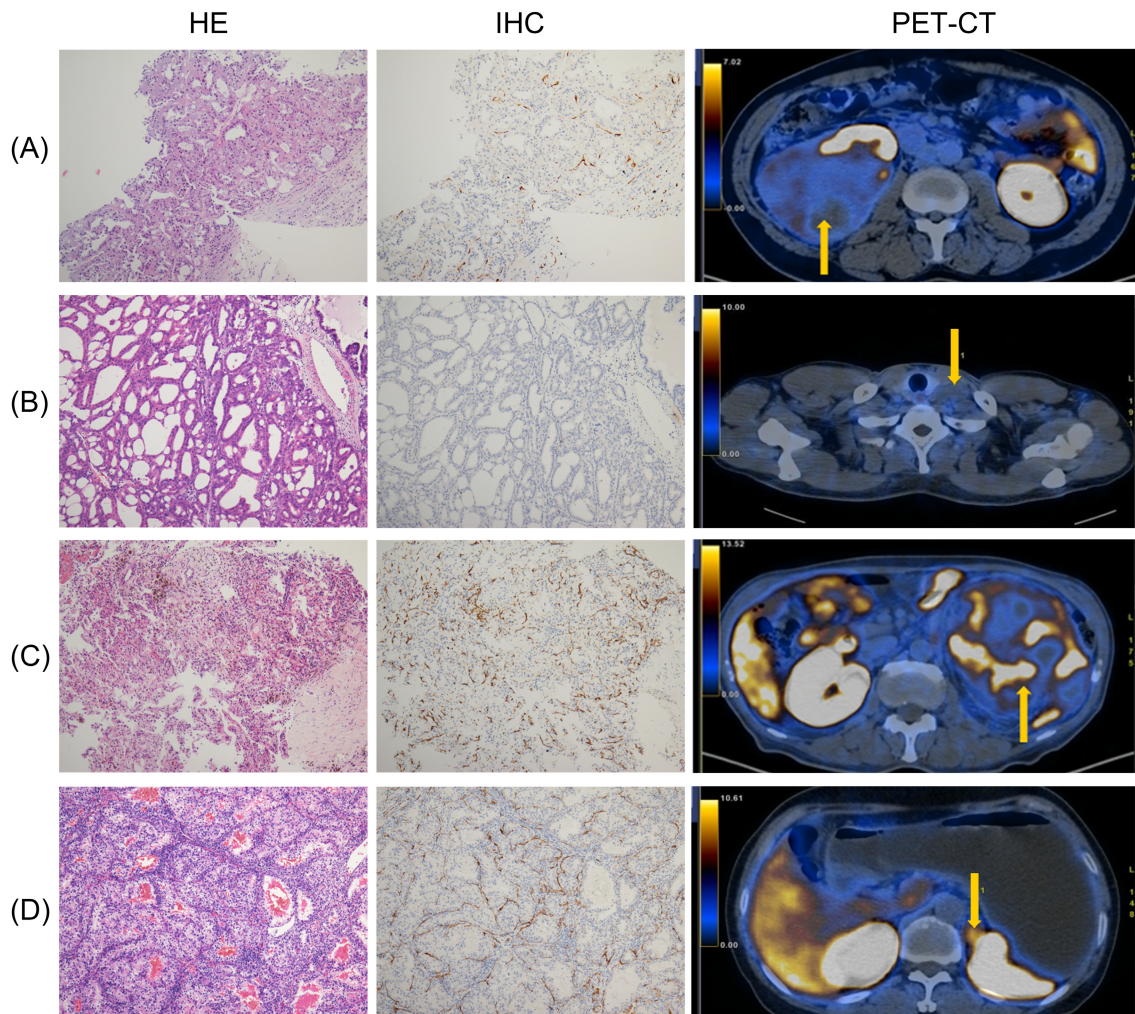
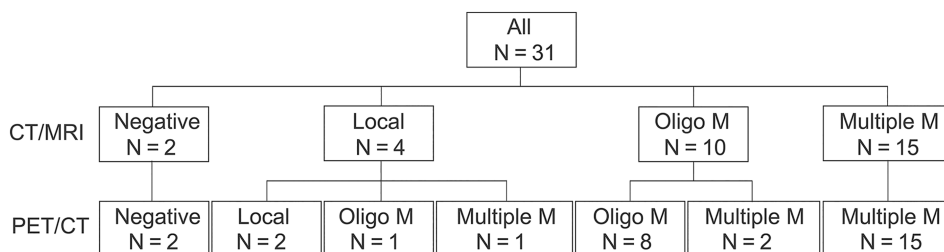


FIGURE 1 Representative images of radio-pathological matching cases. (A) Primary lesion of a patient with ncRCC; (B) metastatic lesion (supraclavicular lymph node) of a patient with ncRCC; (C) primary lesion of a patient with ccRCC; (D) metastatic lesion (adrenal gland) of a patient with ccRCC. ccRCC, clear cell renal cell carcinoma; ncRCC, nonclear cell renal cell carcinoma

FIGURE 2 Per-patient analysis of stage using conventional CT/MRI and ⁶⁸Ga-PSMA-11 PET/CT. CT, computed tomography; ⁶⁸Ga, gallium-68; multiple M, multiple metastases; MRI, magnetic resonance imaging; Oligo M, oligometastases; PSMA, prostate-specific membrane antigen; PET, positron emission tomography



23 patients were diagnosed with ccRCC (Table 1). The numbers of patients diagnosed with localized, oligometastatic and multiple metastatic disease were 4, 10 and 15, respectively, by using conventional imaging, compared with 2, 9 and 18, respectively, by using ⁶⁸Ga-PSMA-11 PET/CT. The management of four patients (12.9%) was changed after detection of new metastases with ⁶⁸Ga-PSMA-11 PET/CT. One patient who was expected to have local recurrence was found with oligometastases. Therefore, the management changed from surgery to radiotherapy. One patient who was expected to have local recurrence was found with multiple metastases. Therefore, the management changed from surgery to medical treatment.

Two patients who were expected to have oligometastases were found to have multiple metastases. Therefore, the management changed from radiotherapy to systemic therapy (Figure 2).

4 | DISCUSSION

To the best of our knowledge, only few case reports and series in which the role of ⁶⁸Ga-PSMA-11 PET/CT in RCC staging have been published.¹⁴⁻²¹ Our aim was to explore the potential use of

^{68}Ga -PSMA-11 PET/CT in the detection of primary and metastatic lesions in different histological subtypes of RCC for the guidance of diagnostic and management decisions compared with conventional imaging. Although this is a small, retrospective study, it contains the largest dataset to date, to our knowledge and the quality of evidence is promising.

The discovery of PSMA expression in RCC dates back to 2007, when Baccala et al³⁰ observed widespread PSMA expression in the endothelial cells of the neovasculature. Positive PSMA staining was detected in 75% to 100% of ccRCC cases, 30% to 73% of chromophobe RCC cases and 0% of papillary RCC cases.^{18,30,31} In our study, the PSMA score of ccRCC was statistically higher than that of ncRCC, and the PSMA score was statistically significantly correlated with the SUV_{max} of the RCC lesions. Thus, we speculate that ^{68}Ga -PSMA-11 PET/CT may be more valuable in ccRCC than in ncRCC. A few case reports and series have been published that indicated that ^{68}Ga -PSMA-11 PET/CT may have advantages in the detection of metastatic lesions of ccRCC.^{16,18,19} To our knowledge, this was the first time that the utilities of ^{68}Ga -PSMA-11 PET/CT in ccRCC and

ncRCC were compared; we discovered that ^{68}Ga -PSMA-11 PET/CT had a better accuracy and sensitivity in the detection of lesions in ccRCC.

Another interesting aspect of our study is the differences that were observed in the TBRs and accuracies of ^{68}Ga -PSMA-11 PET/CT in the detection of lesions from different locations in RCC patients. Some studies have focused on detecting primary RCC.^{17,21,32} In 2021, evaluating 36 ^{68}Ga -PSMA-11 PET/CT scans in primary RCC staging, Gao et al²¹ concluded that the SUV_{max} was high, and the technique could be used to identify aggressive pathological features of primary ccRCC. However, we noticed that the physiological uptake of the surrounding renal parenchyma may be even higher. The addition, TBR, a common indicator of image contrast in PET/CT, may be a better parameter than SUV_{max} alone for the detection. In 2016, Sawicki et al¹⁷ observed that, because of the high uptake in the surrounding renal parenchyma, the mean TBR of the five primary RCCs was only 0.2 ± 0.3 , while that of the metastases was 11.7 ± 0.2 . Similarly, in our study, the median TBR of the lesions in the renal region was 0.33, while those of the metastatic lesions in were 2.13 to 13.71.

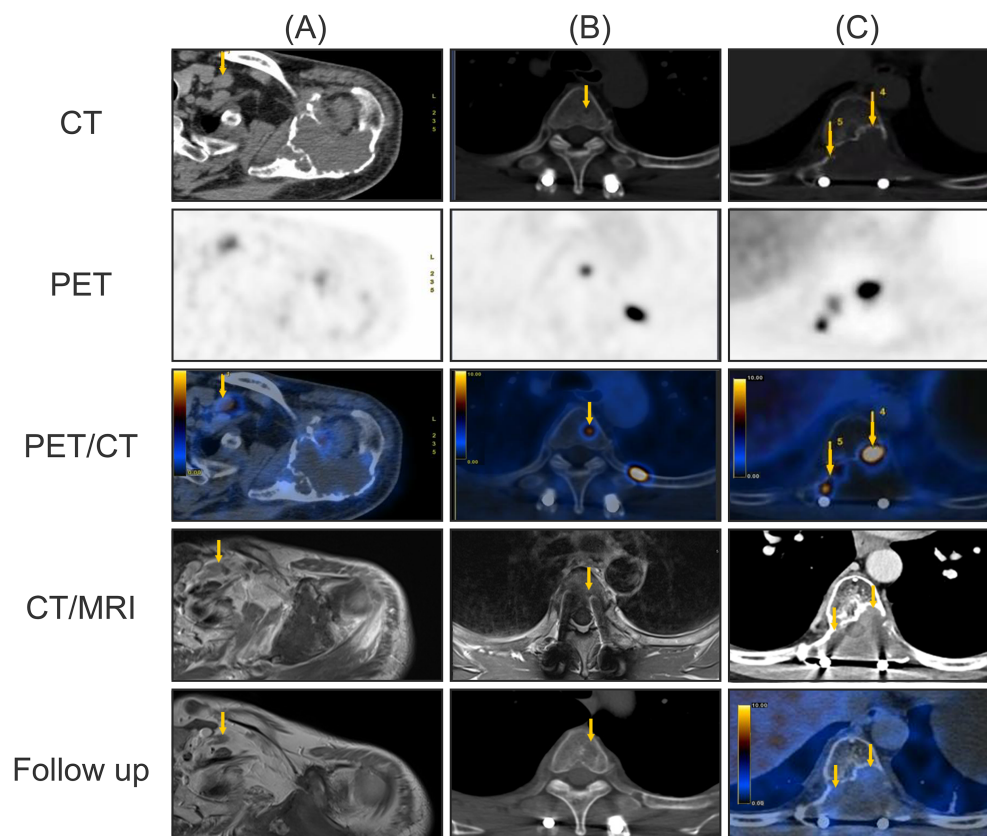


FIGURE 3 Representative images of three patients with baseline conventional imaging and follow-up. (A) ^{68}Ga -PSMA-11 PET/CT revealed a supraclavicular lymph node with increased uptake, which was difficult to diagnose because of its marginal size on conventional MRI. Six-month follow-up MRI following systemic treatment revealed regression of the lymph node. (B) ^{68}Ga -PSMA-11 PET/CT revealed a thoracic vertebral metastasis with increased uptake, which did not appear upon conventional MRI. Twelve-month follow-up MRI after systemic treatment revealed obvious erosive osteoclasia of the thoracic vertebra. (C) ^{68}Ga -PSMA-11 PET/CT revealed a residual thoracic vertebral metastasis after palliative surgery, with increased uptake, which could not be observed upon conventional CT because of metal artifact reduction. Six-month follow-up ^{68}Ga -PSMA-11 PET/CT imaging following radiotherapy revealed a decreased uptake. CT, computed tomography; ^{68}Ga , gallium-68; MRI, magnetic resonance imaging; PET, positron emission tomography; PSMA, prostate-specific membrane antigen

Considering the relatively high detection rate of CT/MRI for primary lesions^{2,3,5} and the difficulty in detecting minor metastases with conventional imaging, we believe that the value of ⁶⁸Ga-PSMA-11 PET/CT lies in the early detection of metastases, as it may promote accurate staging and guide clinical practice.

In the detection of different metastatic lesions in ccRCC, we discovered that ⁶⁸Ga-PSMA-11 PET/CT was more suited to the early detection of lymph node and bone metastases than to that of lung metastases. Evaluation of lymph nodes and bone metastases with CT or MRI solely depends on morphological information, complicating the determination of marginal lymph nodes and small bone metastases.^{12,33} In prostate cancer, a recent meta-analysis demonstrated higher sensitivity (80%) and specificity (97%) for ⁶⁸Ga-PSMA-11 PET/CT in the assessment of lymph node metastases compared with histopathology after salvage lymph node dissection.³⁴ A prospective study of 113 patients revealed that ⁶⁸Ga-PSMA-11 PET/CT had a statistically significantly higher sensitivity and accuracy for the detection of skeletal lesions than did BS (96.2% vs 73.1% and 99.1% vs 84.1%).³⁵ In ccRCC, we discovered that ⁶⁸Ga-PSMA-11 PET/CT is more accurate in the determination of early lymph node metastasis and bone metastasis than conventional imaging (Figure 3A,B). The accuracies of ⁶⁸Ga-PSMA-11 PET/CT in detecting lymph node and bone metastatic lesions in ccRCC were as high as 98.08% and 95.00%, respectively. Moreover, we discovered that ⁶⁸Ga-PSMA-11 PET/CT had advantages in determining whether there were residual tumors after surgery in the form of uptake of contrast agents despite the influence of metal artifacts (Figure 3C). However, the accuracy of ⁶⁸Ga-PSMA-11 PET/CT in the detection of pulmonary metastases was low. Most of the lung metastatic lesions were small, and PET has well-known difficulties in detecting small lung lesions owing to breathing motion and partial volume effects.

The value of accurate imaging is in the guidance it can provide for clinical management of RCC patients. In 2019, Raveenthiran et al¹⁹ noted widespread changes in management after ⁶⁸Ga-PSMA-11 PET/CT in a retrospective case series of 38 patients. Of the 16 patients who underwent ⁶⁸Ga-PSMA-11 PET/CT for primary staging, management was changed in seven (43.8%). Similarly, in our study, ⁶⁸Ga-PSMA-11 PET/CT resulted in a change in management of 12.9% (4/31) of cases because of the discovery of new metastases that were not detected with conventional imaging. The relatively low rate of change of patient management in our study may be because most of our patients already had multiple metastases when they presented with RCC. This suggests that patients with recurrence or oligo-metastases may benefit more from ⁶⁸Ga-PSMA-11 PET/CT than those with multiple metastases.

Our study had several limitations. First, a substantial portion of the patients in our study did not undergo contemporaneous conventional imaging and lacked pathological data, as this was a retrospective study. Second, except for lymph nodes, bone and the lungs, the numbers of other metastatic lesions were too small to be analyzed separately. Third, ccRCC is a group consisting of complex pathological subtypes, but we did not include enough patients for further subgroup analysis. Prospective studies are required to confirm our results.

Considering the paucity of prospective studies and the fact that this retrospective study, despite including only 50 patients, is the largest dataset reported to date, we believe that our study lays the foundation for further exploration of the role of ⁶⁸Ga-PSMA-11 PET/CT in RCC staging. Our data suggest that ⁶⁸Ga-PSMA-11 PET/CT is a promising method for the detection of metastatic lesions in ccRCC patients, especially for metastases in the bone and lymph nodes.

AUTHOR CONTRIBUTIONS

Conceptualization: Pei Dong, Liru He; Formal Analysis: Yilin Li, Rongliang Zheng, Ruiqi Liu; Funding acquisition: Liru He; Methodology: Yilin Li, Rongliang Zheng, Yijun Zhang, Chaoyun Huang, Li Tian, Ruiqi Liu, Yang Liu, Zhiling Zhang, Hui Han, Fangjian Zhou; Resources: Rongliang Zheng, Yijun Zhang, Chaoyun Huang, Li Tian, Ruiqi Liu, Yang Liu, Zhiling Zhang, Hui Han, Fangjian Zhou, Liru He, Pei Dong; Writing—original draft: Yilin Li, Rongliang Zheng, Yijun Zhang; Writing—review & editing Yilin Li, Rongliang Zheng, Yijun Zhang, Liru He, Pei Dong. The work reported in the paper has been performed by the authors, unless clearly specified in the text.

ACKNOWLEDGEMENTS

We acknowledge the financial support of the National Natural Science Foundation of China (Grant number: 81772483) to Dr. Liru He. We also thank Dr. Fan Wei, the chief of Department of Nuclear Medicine, Sun Yat-sen University Cancer Center, for the great help on the support and the Wiley Editing Services for the great help on language.

CONFLICT OF INTEREST

The authors declare no conflict of interest.

DATA AVAILABILITY STATEMENT

The raw imaging data are available at https://figshare.com/articles/figure/PSMA_PET-CT/17696933. Further details and other data that support the findings of this study are available from the corresponding author upon request.

ETHICS STATEMENT

Informed consent was obtained from all individual participants included in the study. Ethics approval was obtained from the Sun Yat-sen University Cancer Center Human Research Ethics Committee (ref.: B2021-233-01). All procedures involving human participants were carried out in accordance with the ethical standards of the institutional research committee and with the 1964 Helsinki Declaration and its later amendments.

ORCID

Ruiqi Liu  <https://orcid.org/0000-0002-2099-620X>

Liru He  <https://orcid.org/0000-0002-7192-0205>

Pei Dong  <https://orcid.org/0000-0001-9749-493X>

REFERENCES

1. Siegel RL, Miller KD, Jemal A. Cancer statistics, 2020. *CA Cancer J Clin.* 2020;70:7-30.

2. Ljungberg B, Bensalah K, Canfield S, et al. EAU guidelines on renal cell carcinoma: 2014 update. *Eur Urol*. 2015;67:913-924.
3. Pedrosa I, Sun MR, Spencer M, et al. MR imaging of renal masses: correlation with findings at surgery and pathologic analysis. *Radiographics*. 2008;28:985-1003.
4. Beuselink B, Pans S, Bielen J, et al. Whole-body diffusion-weighted magnetic resonance imaging for the detection of bone metastases and their prognostic impact in metastatic renal cell carcinoma patients treated with angiogenesis inhibitors. *Acta Oncol*. 2020;59:818-824.
5. Leveridge MJ, Bostrom PJ, Koulouris G, Finelli A, Lawrentschuk N. Imaging renal cell carcinoma with ultrasonography, CT and MRI. *Nat Rev Urol*. 2010;7:311-325.
6. Thompson RH, Hill JR, Babayev Y, et al. Metastatic renal cell carcinoma risk according to tumor size. *J Urol*. 2009;182:41-45.
7. Kinoshita Y, Kuratsukuri K, Landas S, et al. Expression of prostate-specific membrane antigen in normal and malignant human tissues. *World J Surg*. 2006;30:628-636.
8. Salas Fragomeni RA, Amir T, Sheikhabaei S, et al. Imaging of non-prostate cancers using PSMA-targeted radiotracers: rationale, current state of the field, and a call to arms. *J Nucl Med*. 2018;59:871-877.
9. Chang SS, Reuter VE, Heston WD, Gaudin PB. Metastatic renal cell carcinoma neovasculature expresses prostate-specific membrane antigen. *Urology*. 2001;57:801-805.
10. Ahn T, Roberts MJ, Abduljabar A, et al. A review of prostate-specific membrane antigen (PSMA) positron emission tomography (PET) in renal cell carcinoma (RCC). *Mol Imaging Biol*. 2019;21:799-807.
11. Perera M, Papa N, Roberts M, et al. Gallium-68 prostate-specific membrane antigen positron emission tomography in advanced prostate cancer: updated diagnostic utility, sensitivity, specificity, and distribution of prostate-specific membrane antigen-avid lesions: a systematic review and meta-analysis. *Eur Urol*. 2020;77:403-417.
12. Maurer T, Eiber M, Schwaiger M, Gschwend JE. Current use of PSMA-PET in prostate cancer management. *Nat Rev Urol*. 2016;13:226-235.
13. Matushita CS, da Silva AMM, Schuck PN, et al. 68Ga-Prostate-specific membrane antigen (psma) positron emission tomography (pet) in prostate cancer: a systematic review and meta-analysis. *Int Braz J Urol*. 2021;47:705-729.
14. Demirci E, Ocak M, Kabasakal L, et al. (68)Ga-PSMA PET/CT imaging of metastatic clear cell renal cell carcinoma. *Eur J Nucl Med Mol Imaging*. 2014;41:1461-1462.
15. Sasikumar A, Joy A, Nanabala R, Unni M, Tk P. Complimentary pattern of uptake in 18F-FDG PET/CT and 68Ga-prostate-specific membrane antigen PET/CT in a case of metastatic clear cell renal carcinoma. *Clin Nucl Med*. 2016;41:e517-e519.
16. Rhee H, Blazak J, Tham CM, et al. Pilot study: use of gallium-68 PSMA PET for detection of metastatic lesions in patients with renal tumour. *EJNMMI Res*. 2016;6:76.
17. Sawicki LM, Buchbender C, Boos J, et al. Diagnostic potential of PET/CT using a (68)Ga-labelled prostate-specific membrane antigen ligand in whole-body staging of renal cell carcinoma: initial experience. *Eur J Nucl Med Mol Imaging*. 2017;44:102-107.
18. Siva S, Callahan J, Pryor D, Martin J, Lawrentschuk N, Hofman MS. Utility of (68) Ga prostate specific membrane antigen: positron emission tomography in diagnosis and response assessment of recurrent renal cell carcinoma. *J Med Imaging Radiat Oncol*. 2017;61:372-378.
19. Raveenthiran S, Esler R, Yaxley J, Kyle S. The use of (68)Ga-PET/CT PSMA in the staging of primary and suspected recurrent renal cell carcinoma. *Eur J Nucl Med Mol Imaging*. 2019;46:2280-2288.
20. Has Simsek D, Civan C, Erdem S, Sanli Y. Complementary role of 68Ga-prostate-specific membrane antigen and 18F-FDG PET/CT for evaluation of metastases and treatment response in renal cell carcinoma. *Clin Nucl Med*. 2021;46:579-581.
21. Gao J, Xu Q, Fu Y, et al. Comprehensive evaluation of (68)Ga-PSMA-11 PET/CT parameters for discriminating pathological characteristics in primary clear-cell renal cell carcinoma. *Eur J Nucl Med Mol Imaging*. 2021;48:561-569.
22. Yamamoto M, Serizawa T, Shuto T, et al. Stereotactic radiosurgery for patients with multiple brain metastases (JLGG0901): a multi-institutional prospective observational study. *Lancet Oncol*. 2014;15:387-395.
23. Ruers T, Van Coevorden F, Punt CJ, et al. Local treatment of unresectable colorectal liver metastases: results of a randomized phase II trial. *J Natl Cancer Inst*. 2017;109:djx015.
24. Hofman MS, Lawrentschuk N, Francis RJ, et al. Prostate-specific membrane antigen PET-CT in patients with high-risk prostate cancer before curative-intent surgery or radiotherapy (proPSMA): a prospective, randomised, multicentre study. *Lancet*. 2020;395:1208-1216.
25. Dondi F, Albano D, Bertagna F, Giubbini R. Tumor markers and (18)F-FDG PET/CT after orchiectomy in seminoma: is there any correlation? *Rev Esp Med Nucl Imagen Mol (Engl Ed)*. 2021;40:287-292.
26. Ali SA, Amin DH, Abdelkhalek YI. Efficiency of whole-body 18F-FDG PET CT in detecting the cause of rising serum AFP level in post-therapeutic follow-up for HCC patients. *Jpn J Radiol*. 2020;38:472-479.
27. Giesel FL, Kratochwil C, Schlittenhardt J, et al. Head-to-head intra-individual comparison of biodistribution and tumor uptake of (68)Ga-FAPI and (18)F-FDG PET/CT in cancer patients. *Eur J Nucl Med Mol Imaging*. 2021;48:4377-4385.
28. Moch H, Cubilla AL, Humphrey PA, Reuter VE, Ulbright TM. The 2016 WHO classification of Tumours of the urinary system and male genital organs-part a: renal, penile, and testicular Tumours. *Eur Urol*. 2016;70:93-105.
29. Al-Ahmadie HA, Olgac S, Gregor PD, et al. Expression of prostate-specific membrane antigen in renal cortical tumors. *Mod Pathol*. 2008;21:727-732.
30. Baccala A, Sercia L, Li J, Heston W, Zhou M. Expression of prostate-specific membrane antigen in tumor-associated neovasculature of renal neoplasms. *Urology*. 2007;70:385-390.
31. Pozzessere C, Bassanelli M, Ceribelli A, et al. Renal cell carcinoma: the oncologist asks, can PSMA PET/CT answer? *Curr Urol Rep*. 2019;20:68.
32. Golan S, Aviv T, Groshar D, et al. Dynamic (68)Ga-PSMA-11 PET/CT for the primary evaluation of localized renal mass: a prospective study. *J Nucl Med*. 2021;62:773-778.
33. Perera M, Papa N, Christidis D, et al. Sensitivity, specificity, and predictors of positive (68)Ga-prostate-specific membrane antigen positron emission tomography in advanced prostate cancer: a systematic review and meta-analysis. *Eur Urol*. 2016;70:926-937.
34. van Leeuwen PJ, Emmett L, Ho B, et al. Prospective evaluation of ⁶⁸Gallium-prostate-specific membrane antigen positron emission tomography/computed tomography for preoperative lymph node staging in prostate cancer. *BJU Int*. 2017;119:209-215.
35. Lengana T, Lawal IO, Boshomane TG, et al. (68)Ga-PSMA PET/CT replacing bone scan in the initial staging of skeletal metastasis in prostate cancer: a fait accompli? *Clin Genitourin Cancer*. 2018;16:392-401.

SUPPORTING INFORMATION

Additional supporting information can be found online in the Supporting Information section at the end of this article.

How to cite this article: Li Y, Zheng R, Zhang Y, et al. Special issue "The advance of solid tumor research in China": 68Ga-PSMA-11 PET/CT for evaluating primary and metastatic lesions in different histological subtypes of renal cell carcinoma. *Int J Cancer*. 2023;152(1):42-50. doi:10.1002/ijc.34189